

# Bispectral analysis of nonlinear compressional waves in a two-dimensional dusty plasma crystal

V. Nosenko,\* J. Goree, and F. Skiff

*Department of Physics and Astronomy, The University of Iowa, Iowa City, Iowa 52242, USA*

(Received 30 August 2005; published 3 January 2006)

Bispectral analysis was used to study the nonlinear interaction of compressional waves in a two-dimensional strongly coupled dusty plasma. A monolayer of highly charged polymer microspheres was suspended in a plasma sheath. The microspheres interacted with a Yukawa potential and formed a triangular lattice. Two sinusoidal pump waves with different frequencies were excited in the lattice by pushing the particles with modulated  $\text{Ar}^+$  laser beams. Coherent nonlinear interaction of the pump waves was shown to be the mechanism of generating waves at the sum, difference, and other combination frequencies. However, coherent nonlinear interaction was ruled out for certain combination frequencies, in particular, for the difference frequency below an excitation-power threshold, as predicted by theory.

DOI: [10.1103/PhysRevE.73.016401](https://doi.org/10.1103/PhysRevE.73.016401)

PACS number(s): 52.27.Lw, 82.70.Dd, 52.35.Mw, 52.27.Gr

## I. INTRODUCTION

Bispectral analysis is a powerful tool to study nonlinear phenomena [1]. In this method, a correlation is calculated between fluctuations at different frequencies in Fourier spectra of the waves studied. If the correlation among a triplet of waves at frequencies  $F_1$ ,  $F_2$ , and  $F_1+F_2$  is strong, this result indicates phase coupling between these waves. In this case, the wave at  $F_1+F_2$  is a result of coherent nonlinear interaction of waves at  $F_1$  and  $F_2$ . If there is no correlation in the triplet  $F_1$ ,  $F_2$ , and  $F_1+F_2$ , this rules out the coherent nonlinear interaction of waves at  $F_1$  and  $F_2$ .

In this paper, we use bispectral analysis to clarify questions that remained unresolved in Ref. [2]. In that paper, an experiment was reported where nonlinear three-wave interaction of compressional waves was observed in a two-dimensional (2D) dusty plasma.

A dusty plasma is a suspension of micron-sized particles in a plasma. The particles are highly charged, and due to mutual repulsion in combination with the natural confinement provided by the plasma's radial electric field, they arrange themselves in a structure, called a plasma crystal, with crystalline or liquidlike order. In the presence of gravity, particles can settle in a 2D monolayer, whereas the plasma's electrons and ions fill a three-dimensional (3D) volume. The particles can be imaged directly, and their positions and velocities calculated, which allows studying the lattice microscopically.

Sound waves, or phonons, are well-studied in the linear or low-amplitude limit. The literature, both theoretical and experimental, for 2D dusty plasmas is reviewed in Ref. [3] and references cited therein.

The properties of nonlinear waves in dusty plasmas have also been studied, but not as completely as for linear waves. It was shown theoretically that nonlinear pulses can take the form of solitons in weakly [4] and strongly coupled [5–7] dusty plasmas, although frictional gas damping can suppress soliton formation [6,7]. In experiments with large ampli-

tudes, nonlinear pulses [5,8] and harmonic generation [2,9] were observed in 2D lattices. Harmonic generation was explained theoretically in Refs. [9,10].

## II. REVIEW OF EXPERIMENT

In this paper we will present further analysis, using different methods, of the experiment of Nosenko *et al.* [2], where nonlinear mixing of compressional waves was observed in a 2D dusty plasma crystal. Below, we will briefly review the experimental procedure and main results of Ref. [2].

A monolayer of highly charged polymer microspheres was suspended in a plasma sheath, Fig. 1. The particle suspension had a diameter of about 60 mm. The particles had a diameter of  $8.09 \pm 0.18 \mu\text{m}$  [11] and a mass density  $1.514 \text{ g/cm}^3$ . To achieve a low damping rate, Ar gas was used at a pressure of 5 mTorr, so that the gas drag, which is accurately modeled [11] by the Epstein expression, was only  $\nu_d = 0.87 \text{ s}^{-1}$ . The plasma was sustained by a 13.56 MHz rf voltage with a peak-to-peak amplitude of 168 V and a self-bias of  $-115 \text{ V}$ .

The particles in the suspension arranged themselves in a triangular lattice, as shown in the image in Fig. 1(a). The interparticle spacing was  $a = 675 \pm 14 \mu\text{m}$ , as identified by the first peak in the pair correlation function  $g(r)$ . The lattice was in an ordered state;  $g(r)$  had many peaks, and it had translational order length of  $16a$  in an undisturbed lattice, although this diminished to  $4a$  when large-amplitude waves were excited. A pulse technique [12] making use of a theoretical wave dispersion relation was used to measure the particle charge  $Q = -9400 \pm 900e$  and screening length  $\lambda_D = 0.73 \pm 0.1 \text{ mm}$  at the particles' height.

The particles were imaged through the top window by a video camera, and they were illuminated by a horizontal He-Ne laser sheet. Movies of 68.3–136.7 s duration were digitized using a digital VCR at 29.97 frames per second. The  $24 \times 18 \text{ mm}$  field of view included 1000–1100 particles, Fig. 1(a). Particle coordinates and velocities were then calculated in each frame using the moment method [13]. The  $x$ - $y$  coordinate system in the plane of particle suspension has

\*Electronic address: [vladimir-nosenko@uiowa.edu](mailto:vladimir-nosenko@uiowa.edu)

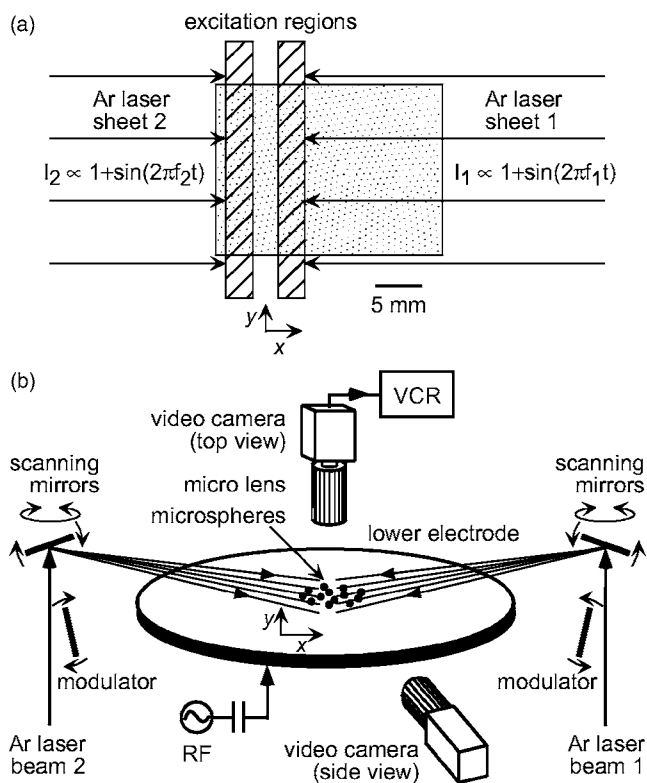


FIG. 1. Experimental apparatus. (a) Particles arranged in a triangular 2D lattice. Atop this image is a sketch showing where the radiation pressure force from two modulated Ar<sup>+</sup> laser sheets pushes particles, exciting sinusoidal compressional pump waves. (b) The particles are polymer microspheres, suspended as a monolayer above the lower electrode in a capacitively coupled rf plasma. All our analysis is based on images recorded by the top-view camera.

its  $x$  axis in the direction of the laser beam, as shown in Fig. 1(b), so that waves propagated in the  $\pm x$  directions.

A laser-manipulation method was used to excite two sinusoidal compressional pump waves with different frequencies,  $f_1=0.7$  Hz and  $f_2=1.7$  Hz, and parallel wave fronts in the plasma crystal, Fig. 1. Particles were pushed by the radiation pressure force, which is proportional to an incident laser intensity [11]. Measurements were repeated with three different laser powers to vary the pump strength, and also with no laser power. We will report the laser power as measured inside the vacuum chamber. Our highest power was 3.41 W. Note that this power was distributed over a narrow rectangular stripe that traversed the particle suspension. To understand how large the pump power was, the most physically significant parameter is the peak velocity of the particles in the stripe where the laser struck. This peak velocity was 0.72 mm/s, corresponding to 3.3% of the sound speed for compressional waves, at our highest laser power of 3.41 W.

The results of this experiment as reported in Ref. [2] were observations of the waves propagating in the lattice at the sum, difference, and other combination frequencies, as well as harmonics of the pump waves. The waves at the sum frequencies  $f_1+f_2$  and  $2f_1+f_2$  were found to be generated only above an excitation-power threshold. This threshold

was attributed to frictional damping, as predicted by nonlinear wave theory [2].

### III. ANALYSIS METHOD

In the present paper, we use a different method, bispectral analysis, to clarify the mechanism of generating waves at different combination frequencies in the experiment of Ref. [2]. We performed bispectral analysis of the particle velocity using the following procedure. The  $x$  component of the particle velocity was spatially averaged within 40 rectangular bins elongated along the  $y$  axis. The fast Fourier transform  $v_x(f)$  of the averaged particle velocity  $v_x(t)$  was then computed for each of the 40 bins. Then we calculated the maps of the squared bicoherence,

$$\gamma^2(F_1, F_2) = \frac{|\langle v_x(F_1)v_x(F_2)v_x^*(F_1 + F_2) \rangle|^2}{\langle |v_x(F_1)v_x(F_2)|^2 \rangle \langle |v_x(F_1 + F_2)|^2 \rangle}, \quad (1)$$

where  $\langle \dots \rangle$  denotes the ensemble average and  $v_x^*$  is the complex conjugate of  $v_x$ . Ensemble averaging was performed in nine data bins that were located 6.5–11.1 mm away from the excitation region. The amplitudes of waves at combination frequencies did not change significantly between these data bins. In addition, the 4096-frame time sequence of  $v_x(t)$  in each of these bins was divided into four 1024-frame subsequences. Thus we obtained  $n=36$  ensembles, each 1024 frames long, to calculate the ensemble average. The length of each ensemble was enough to calculate  $v_x(f)$  with sufficient frequency resolution.

The aim of using bispectral analysis is to determine whether there is significant coupling between three waves, as indicated by a strong correlation. It is customary to characterize the coupling as strong if  $\gamma^2$  is nearly unity and absent if it is near zero [14]. Coupling that is not strong can nevertheless be deemed statistically significant at the 95% confidence level if  $\gamma^2 > 3/n$ , which for our case is  $\gamma^2 > 0.083$ [15]. We will test three different experimental cases, corresponding to three different pump power levels, and we will find that strong coupling, with  $\gamma^2$  near unity, occurs in two of these cases, for the experiment of Ref. [2].

### IV. RESULTS

#### A. Compressional waves

Going beyond the power spectra reported in Ref. [2], we also present two other kinds of maps. These are maps of the bicoherence  $\gamma^2(F_1, F_2)$  and maps of the wave energy in  $\omega$ - $k$  space. The maps of  $\gamma^2$  are presented as functions of two independent variables,  $F_1$  and  $F_2$ ; these should not be confused with  $f_1$  and  $f_2$ , which represent the two pump frequencies in the experiment. The bicoherence maps indicate whether a coherent nonlinear coupling occurs amongst three oscillations. Whether these oscillations correspond to a propagating wave or some other oscillation such as a sloshing mode is revealed by the energy maps in  $\omega$ - $k$  space. The maps of bicoherence and of energy in  $\omega$ - $k$  space were not previously reported in Ref. [2] for the same experiment.

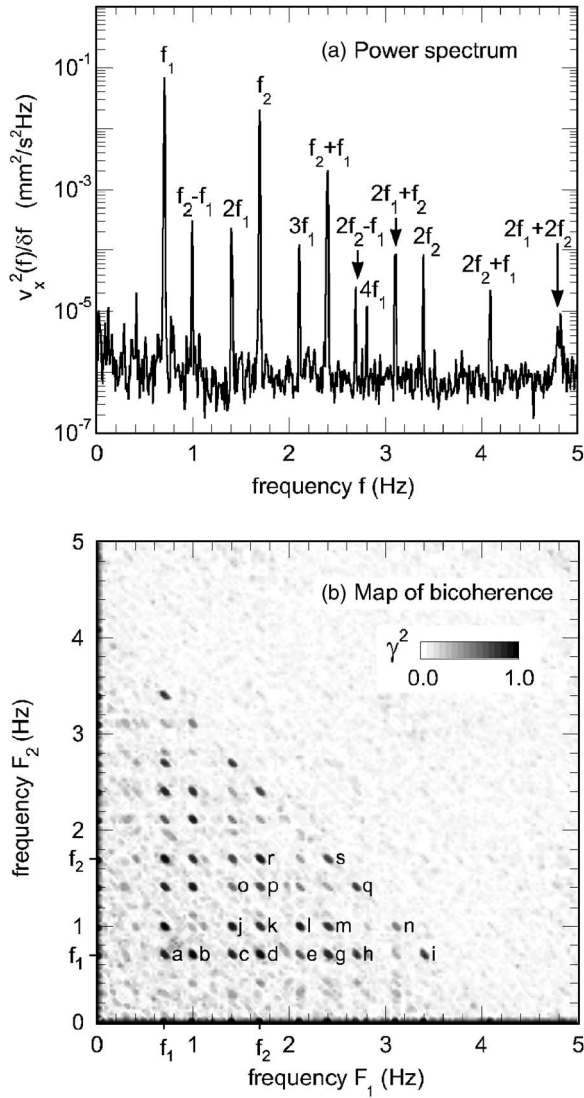


FIG. 2. (a) Power spectrum  $|v_x(f)|^2$  and (b) map of the squared bicoherence  $\gamma^2(F_1, F_2)$  of the particle velocity. Note that  $f$ ,  $F_1$ , and  $F_2$  denote independent variables, whereas  $f_1=0.7$  Hz and  $f_2=1.7$  Hz are the pump frequencies. Data shown here are for a high excitation laser power of 3.41 W. In (b), a dark color indicates a high bicoherence,  $\gamma^2(F_1, F_2) \approx 1$ ; when this occurs, the waves at frequencies  $F_1$ ,  $F_2$ , and  $F_1+F_2$  are not only harmonically related, but phase coupled as well, which is a signature of coherent nonlinear interaction between the waves at  $F_1$  and  $F_2$ . Interpretation of all peaks labeled in (b) is presented in Table I. Note that the map of bicoherence is symmetric relative to the line  $F_1=F_2$ , since  $\gamma^2(F_1, F_2) = \gamma^2(F_2, F_1)$ .

At our highest amplitude for the pump waves, with a laser power of 3.41 W, the power spectrum of particle velocity has peaks corresponding to the pump waves, their harmonics, and waves at various combination frequencies, as shown in Fig. 2(a). This figure is similar to Fig. 2a of Ref. [2], except that in the present paper the power spectrum was calculated in the same region of the plasma crystal located 6.5–11.1 mm away from the excitation region that was used to calculate bicoherence. Next, we examine our results for

the two other kinds of maps, bicoherence and wave energy in  $\omega$ - $k$  space.

The map of squared bicoherence  $\gamma^2$  in Fig. 2(b) shows that the waves at combination frequencies are a result of coherent nonlinear interaction of the pump waves, thus supporting a similar conclusion made in Ref. [2]. The black dots in this map indicate the pairs of frequencies  $F_1$ ,  $F_2$ , where the squared bicoherence  $\gamma^2(F_1, F_2)$  is nearly unity, indicating strong coupling. For any point on the map where  $\gamma^2$  is near unity, we conclude that the corresponding frequencies  $F_1$ ,  $F_2$ , and  $F_1+F_2$  are not only harmonically related, but phase coupled as well, which is a signature of coherent nonlinear interaction between the waves at  $F_1$  and  $F_2$ . Note that the map is symmetric relative to the line  $F_1=F_2$ , since  $\gamma^2(F_1, F_2) = \gamma^2(F_2, F_1)$ .

We identify peaks corresponding to at least 12 nonlinear interactions at combination frequencies in Fig. 2(b). We list these in Table I. We also list peaks that are ambiguous because we are unable to definitively identify their generation mechanism. Among the 12 peaks that we can explain are the generation of combination frequencies  $f_1+f_2$ ,  $f_2-f_1$ ,  $2f_1+f_2$ , and  $2f_2-f_1$ . For example, for the point (0.7 Hz, 1.7 Hz) on the map corresponding to our two pump frequencies, the value of the squared bicoherence is near unity,  $\gamma^2(f_1, f_2) = 0.954$ . This peak shows that a third wave exists with a frequency  $f_1+f_2=2.4$  Hz, and that the phase of this wave equals  $\phi_1+\phi_2$ , where  $\phi_1$  and  $\phi_2$  are the phases of the waves at  $f_1$  and  $f_2$ . For this example, one can conclude that the generation mechanism for the sum-frequency wave is coherent nonlinear interaction of the pump waves. As another example, for the point (1 Hz, 0.7 Hz) the squared bicoherence is also near unity. This means that the three waves with frequencies  $f_2-f_1=1$  Hz,  $f_1$ , and  $f_2$  are phase coupled. We interpret this finding as evidence that the difference-frequency wave is generated by coherent nonlinear interaction of the pump waves, at this high level of excitation laser power.

We will now compare the map of squared bicoherence  $\gamma^2$  in Fig. 2(b) and the power spectrum  $|v_x(f)|^2$  for particle motion in Fig. 2(a). Each peak at a combination frequency in the power spectrum in Fig. 2(a) has one or more corresponding peaks in the bicoherence map in Fig. 2(b). The latter peaks show different ways the wave at that combination frequency was generated. There is one exception, though. For the peak at  $2f_1+2f_2=4.8$  Hz in Fig. 2(a), there is no corresponding peak in Fig. 2(b). We will discuss the significance of this finding for the wave at 4.8 Hz later in this paper.

At our medium amplitude for the pump waves, with a laser power of 1.19 W, the power spectrum of particle velocity has fewer peaks, in Fig. 3(a). Some combination-frequency peaks have disappeared at this lower amplitude, as compared to the higher amplitude case of Fig. 2. This occurs because the pump amplitude became lower than the threshold value, as explained by the theory of Ref. [2]. Remaining peaks at the combination frequencies of  $f_2-f_1$ ,  $f_1+f_2$ , and  $2f_1+f_2$  are still a result of coherent nonlinear interaction of the pump waves, as indicated by corresponding peaks in the map of bicoherence in Fig. 3(b), where  $\gamma^2$  is near unity. For example, at the point corresponding to our two pump frequencies, the squared bicoherence is  $\gamma^2(f_1, f_2) = 0.957$ .

TABLE I. Frequencies and physical significance of the peaks in bicoherence in Figs. 2(b) and 3(b). The two pump frequencies are  $f_1=0.7$  Hz and  $f_2=1.7$  Hz.

Peak	$F_1$ (Hz)	$F_2$ (Hz)	$F_1+F_2$ (Hz)	combination frequency
<i>Interpretation: coherent nonlinear generation of combination frequencies</i>				
<i>a</i>	0.7	0.7	1.4	second harmonic of $f_1$
<i>b</i>	1.0	0.7	1.7	difference frequency $f_2-f_1=1$ Hz
<i>c</i>	1.4	0.7	2.1	third harmonic of $f_1$
<i>d</i>	1.7	0.7	2.4	sum frequency $f_1+f_2$
<i>e</i>	2.1	0.7	2.8	fourth harmonic of $f_1$
<i>g</i>	2.4	0.7	3.1	sum frequency $2f_1+f_2$
<i>h</i>	2.7	0.7	3.4	difference frequency $2f_2-f_1=2.7$ Hz
<i>i</i>	3.4	0.7	4.1	sum frequency $f_1+2f_2$
<i>o</i>	1.4	1.4	2.8	fourth harmonic of $f_1$
<i>p</i>	1.7	1.4	3.1	sum frequency $2f_1+f_2$
<i>r</i>	1.7	1.7	3.4	second harmonic of $f_2$
<i>s</i>	2.4	1.7	4.1	sum frequency $f_1+2f_2$
<i>Interpretation is ambiguous</i>				
<i>j</i>	1.4	1	2.4	
<i>k</i>	1.7	1	2.7	
<i>l</i>	2.1	1	3.1	
<i>m</i>	2.4	1	3.4	
<i>n</i>	3.1	1	4.1	
<i>q</i>	2.7	1.4	4.1	

At our lowest amplitude of the pump waves, with a laser power of 0.11 W, the power spectrum of particle velocity in Fig. 4(a) has, besides the pump frequencies, two peaks at the combination frequencies  $f_2-f_1=1$  Hz and  $2f_1+2f_2=4.8$  Hz, and lower peaks at frequencies that seem to be unrelated to the pump frequencies. However, there are no peaks with  $\gamma^2$  near unity in the corresponding map of bicoherence in Fig. 4(b). We summarize these observations in Table II. For example, at the point corresponding to our two pump frequencies, the squared bicoherence is  $\gamma^2(f_1, f_2)=0.022$ . This means that there is no coherent nonlinear interaction of the pump waves when they have low amplitude, in agreement with the theory of Ref. [2]. The origin of the peaks at 1 Hz and 4.8 Hz in Fig. 4(a) thus remains unclear. We will discuss the waves at 1 Hz and 4.8 Hz later in this paper.

One of the chief results of this paper is that using bispectral analysis verifies the theoretical prediction of Ref. [2] of an excitation-power threshold for the generation of a difference-frequency wave. The peak at the difference frequency  $f_2-f_1=1$  Hz is present in the power spectra of the particle velocity at all values of laser power, as shown in Figs. 2(a), 3(a), and 4(a). However, the corresponding peaks in the respective maps of bicoherence are only present at the two higher values of laser power, Figs. 2(b) and 3(b). Compare, for example, Figs. 3 and 4. The peak at 1 Hz is present in the power spectra in Figs. 3(a) and 4(a), with similar amplitudes, yet the corresponding peak in the map of bicoherence is only present in Fig. 3(b). In general, the peak at 1 Hz is present in the maps of bicoherence at laser powers of 1.19 W and higher, while it is missing at laser powers of 0.61 W and below. This means that the wave

at  $f_2-f_1=1$  Hz is phase coupled to the pump waves for  $P_{\text{laser}} \geq 1.19$  W, but it is not phase coupled to the pump waves for  $P_{\text{laser}} \leq 0.61$  W. Hence the wave at 1 Hz can be attributed to coherent nonlinear mixing of the pump waves only at higher values of laser power  $P_{\text{laser}} \geq 1.19$  W, in agreement with the prediction of theory of Ref. [2] that there is an excitation-power threshold for generation of combination-frequency waves.

Similarly, bispectral analysis helps to reveal that the peak at 4.8 Hz in the power spectra of the particle velocity is not a result of coherent nonlinear mixing of the pump waves regardless of their amplitude, even though this peak happens to be at the combination frequency  $2f_1+2f_2$ . Indeed, the phase of the wave at 4.8 Hz is not coupled to the phases of the pump waves, as evidenced by the absence of the corresponding peaks in the maps of bicoherence in Figs. 2(b) and 4(b).

## B. Other oscillations

While bispectral analysis can tell us that the waves at  $f_2-f_1=1.0$  Hz (below the excitation-power threshold) and  $2f_1+2f_2=4.8$  Hz are not a result of coherent nonlinear mixing of the pump waves, it cannot tell us what they are. In particular, it cannot tell us whether the observed oscillations are propagating waves. For that purpose, we need an additional method, described next.

A more complete identification of observed oscillations can be obtained from the analysis of the map of wave energy in  $\omega$ - $k$  space shown in Fig. 5. The wave energy is mostly concentrated in distinct peaks that correspond to the pump

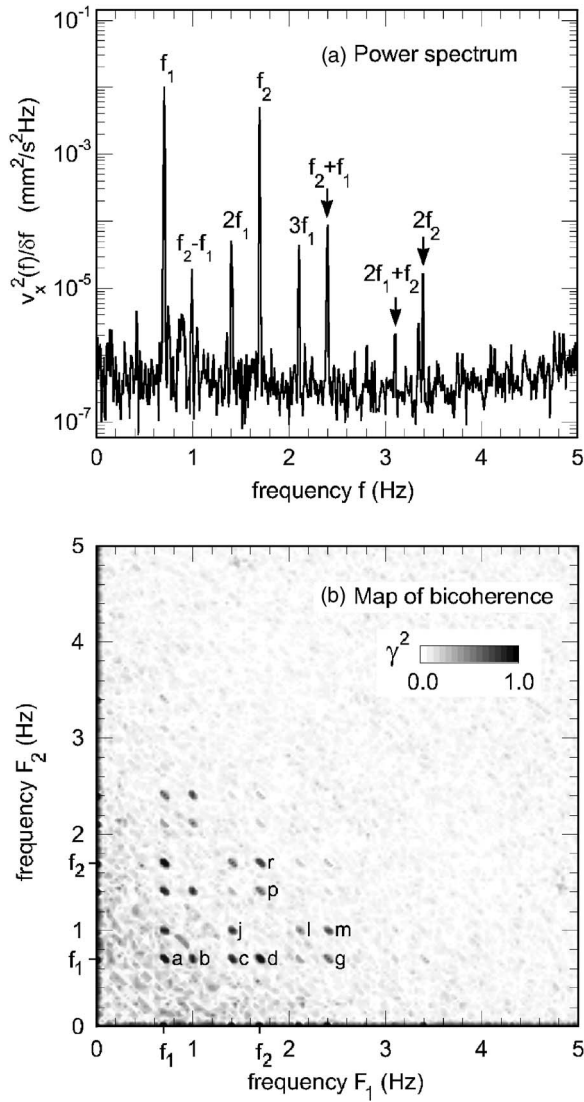


FIG. 3. (a) Power spectrum  $|v_x(f)|^2$  and (b) map of the squared bicoherence  $\gamma^2(F_1, F_2)$  of the particle velocity for the medium excitation laser power of 1.19 W. Interpretation of all peaks labeled in (b) is presented in Table I.

waves, their harmonics, and waves at combination frequencies. These peaks are superimposed on weaker curved stripes representing the dispersion relation of spontaneously excited compressional waves, as observed in the experiment in Ref. [16]. However, some peaks in Fig. 5 do not lie on the dispersion relation. Most notably, the oscillations at 4.8 Hz and 6.3 Hz have a wave number  $k \approx 0$ . These are therefore close to a sloshing mode, i.e., a motion of all particles together as a rigid body in the confining potential provided by the plasma's radial electric field [17]. Such an oscillation does not satisfy the compressional wave's dispersion relation. This observation supports the conclusion made earlier that the oscillation at 4.8 Hz is not generated by coherent nonlinear mixing of the pump waves. Therefore, it is only a coincidence that this oscillation happens to be at the combination frequency  $2f_1 + 2f_2 = 4.8$  Hz. It may be excited by a spontaneous motion of a lattice defect or an energetic particle beneath the monolayer [18]. It may also be an artifact due to

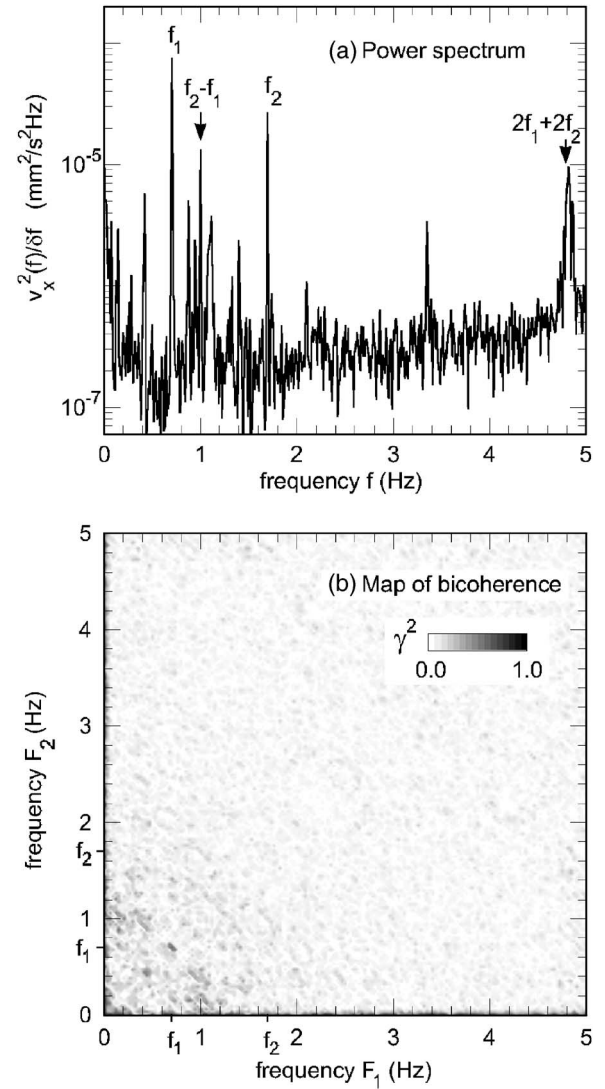


FIG. 4. (a) Power spectrum  $|v_x(f)|^2$  and (b) map of the squared bicoherence  $\gamma^2(F_1, F_2)$  of the particle velocity for the low excitation laser power of 0.11 W. Although the power spectrum has peaks at combination frequencies  $f_2 - f_1 = 1$  Hz and  $2f_1 + 2f_2 = 4.8$  Hz, the bicoherence has no peaks that would indicate strong coupling, i.e.,  $\gamma^2 \ll 1$  for all frequencies. This rules out coherent nonlinear interaction of the pump waves at this low amplitude. Observation of combination frequencies present in power spectra but absent in bicoherence maps is summarized in Table II.

camera vibration or noise in the camera and electronics. This oscillation at 4.8 Hz might indeed be intermittent, because it is absent for the data series presented in Fig. 3.

Similarly, the oscillation at 1 Hz has a wave number  $k \approx 0$  at our lowest amplitude, which is below the excitation-

TABLE II. Combination frequencies with peaks in power spectra but absent in bicoherence maps.

peak	combination frequency	comments
4.8 Hz	$2f_1 + 2f_2$	always absent
1 Hz	$f_2 - f_1$	absent at low pump amplitude

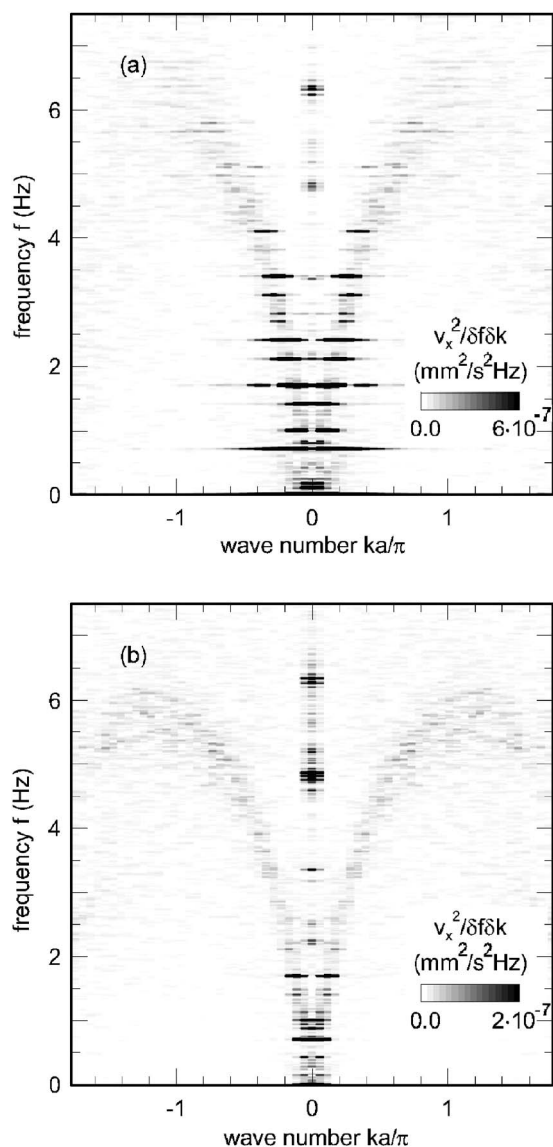


FIG. 5. Map of wave energy in  $\omega$ - $k$  space for (a) high and (b) low excitation laser power. The levels of laser power in (a) and (b) correspond to Figs. 2 and 4, respectively. The wave energy is mostly concentrated in distinct peaks that correspond to the pump waves, their harmonics, and waves at combination frequencies. These peaks are superimposed on weaker stripes representing the dispersion relation of spontaneously excited compressional waves [16]. The oscillation at 4.8 Hz has a wave number  $k \approx 0$  and does not satisfy the dispersion relation. This oscillation is not generated by coherent nonlinear interaction of the pump waves, even though it happens to be at the frequency  $2f_1 + 2f_2 = 4.8$  Hz.

power threshold, Fig. 5(b). This means that below the excitation-power threshold, this oscillation, as in the case of 4.8 Hz, is a long-wavelength motion of particles probably caused by oscillating defects or particles beneath the monolayer. On the other hand, above the excitation-power threshold, the wave at 1 Hz has a finite wave number  $k \neq 0$ , that lies on the dispersion relation of compressional waves, as shown in Fig. 5(a). This supports the conclusion that the difference-frequency wave is generated by coherent nonlin-

ear mixing of the pump waves, above the excitation-power threshold.

Finally, we note some faint unexplained features in the map of bicoherence for the lowest pump amplitude, Fig. 4(b). Even though there is no coherent nonlinear interaction of the pump waves when they have low amplitudes, the map of bicoherence in Fig. 4(b) has peaks at random frequencies in the range  $F_{1,2} \leq 1$  Hz. These peaks are weak, with a squared bicoherence of only  $\gamma^2 \leq 0.4$ . The frequencies of these random peaks, however, are unrelated to the pump frequencies. Similar peaks with  $\gamma^2 \leq 0.3$  are present even without any external excitation (zero pump amplitude). These bicoherence levels indicate that the coupling is not strong, although they might be statistically significant. The latter observation might be an indication of phase coupling between spontaneously excited low-frequency long-wavelength waves in a 2D plasma crystal. On the other hand, these features at low amplitude might also be merely artifacts of the random errors in our velocity measurements.

## V. USES OF BISPECTRAL ANALYSIS BEYOND BICOHERENCE

Bispectral analysis can provide more information on nonlinear wave interaction than is illustrated in this paper. Rather than use the bicoherence  $\gamma^2$ , one could use the bispectrum

$$B(F_1, F_2) = \langle v_x(F_1)v_x(F_2)v_x^*(F_1 + F_2) \rangle, \quad (2)$$

where we have used the same notations as in Eq. (1). It can be shown that the imaginary part of the bispectrum carries information on the rate of power transfer between different modes. This method will be described in detail elsewhere.

## VI. SUMMARY

We showed how bispectral analysis can be used to study nonlinear interaction of waves in an externally driven system. In bispectral analysis, the value of bicoherence  $\gamma^2$  between different modes measures the strength of coupling between these modes. Bispectral analysis provides a deeper insight into the nature of the nonlinear wave generation mechanism than is possible using the usual power spectrum, because, unlike a power spectrum, bicoherence carries information on the phase relations between modes. Analysis of bicoherence can therefore help to distinguish between coherent nonlinear generation of combination-frequency waves and other generation mechanisms. In our experiment with a plasma crystal, where two pump waves at different frequencies were externally excited, we showed how analysis of bicoherence is useful in two ways. First, it confirms that a certain combination frequency is indeed a result of coherent nonlinear interaction of pump waves, if we observe  $\gamma^2 \approx 1$  for that combination frequency. Second, it rules out coherent nonlinear interaction, if we observe  $\gamma^2 \ll 1$ . In particular, we showed that the difference-frequency wave was generated by coherent nonlinear interaction of pump waves above an excitation-power threshold, and by some other mechanism

below the threshold. This supports the theoretical prediction of Ref. [2] about the existence of an excitation-power threshold, for the difference-frequency wave. Finally, further uses of bispectral analysis beyond bicoherence were suggested.

#### ACKNOWLEDGMENTS

This work was supported by NASA and the U.S. Department of Energy.

- 
- [1] T. Subba Rao and M. M. Gabr, *Lecture Notes in Statistics: An Introduction to Bispectral Analysis and Bilinear Time Series Models* (Springer-Verlag, New York, 1984), Vol. 24.
  - [2] V. Nosenko, K. Avinash, J. Goree, and B. Liu, *Phys. Rev. Lett.* **92**, 085001 (2004).
  - [3] A. Piel, A. Homann, M. Klindworth, A. Melzer, C. Zafiu, V. Nosenko, and J. Goree, *J. Phys. B* **36**, 533 (2003).
  - [4] N. N. Rao, P. K. Shukla, and M. Y. Yu, *Planet. Space Sci.* **38**, 543 (1990).
  - [5] D. Samsonov, A. V. Ivlev, R. A. Quinn, G. Morfill, and S. Zhdanov, *Phys. Rev. Lett.* **88**, 095004 (2002).
  - [6] S. K. Zhdanov, D. Samsonov, and G. E. Morfill, *Phys. Rev. E* **66**, 026411 (2002).
  - [7] K. Avinash, P. Zhu, V. Nosenko, and J. Goree, *Phys. Rev. E* **68**, 046402 (2003).
  - [8] V. Nosenko, S. Nunomura, and J. Goree, *Phys. Rev. Lett.* **88**, 215002 (2002).
  - [9] S. Nunomura, S. Zhdanov, G. E. Morfill, and J. Goree, *Phys. Rev. E* **68**, 026407 (2003).
  - [10] K. Avinash, *Phys. Plasmas* **11**, 1891 (2004).
  - [11] B. Liu, J. Goree, and V. Nosenko, *Phys. Plasmas* **10**, 9 (2003).
  - [12] V. Nosenko, J. Goree, Z. W. Ma, and A. Piel, *Phys. Rev. Lett.* **88**, 135001 (2002).
  - [13] A. Melzer, S. Nunomura, D. Samsonov, Z. W. Ma, and J. Goree, *Phys. Rev. E* **62**, 4162 (2000).
  - [14] K. Kim and S. Kim, *J. Phys. Soc. Jpn.* **65**, 2323 (1996).
  - [15] R. A. Haubrich, *J. Geophys. Res.* **70**, 1415 (1965).
  - [16] S. Nunomura, J. Goree, S. Hu, X. Wang, A. Bhattacharjee, and K. Avinash, *Phys. Rev. Lett.* **89**, 035001 (2002).
  - [17] S. Nunomura, J. Goree, S. Hu, X. Wang, and A. Bhattacharjee, *Phys. Rev. E* **65**, 066402 (2002).
  - [18] V. A. Schweigert, I. V. Schweigert, V. Nosenko, and J. Goree, *Phys. Plasmas* **9**, 4465 (2002).